

MODELING OF SPLIT RING RESONATOR FOR HARVESTING ELECTROMAGNETIC ENERGY WITH RESONANT FREQUENCY OF 950 MHZ

^{1,*}Ahmad Raditya C Baswara, ²F Danang Wijaya, ³Eka Firmansyah, ⁴Tua Raja Simbolon, ⁵Berthianna Nurcresia

¹Department of Electrical Engineering, Universitas Ahmad Dahlan, Yogyakarta

²Department of Electrical Engineering and Information Technology, Universitas Gadjah Mada, Yogyakarta

³Department of Electrical Engineering and Information Technology, Universitas Gadjah Mada, Yogyakarta

⁴ Department of Physics, Universitas Sumatera Utara, Medan

⁵ Department of Physics, Universitas Sumatera Utara, Medan

e-mail: ^{1,*}ahmad.baswara@te.uad.ac.id, ²danangwijaya@ugm.ac.id ³eka.firmansyah@ugm.ac.id,

⁴tuaraja@usu.ac.id, ⁵berthiflynn@gmail.com

*Correspondence author

Abstract

The use of a split ring resonator (SRR) as an electromagnetic energy harvester can increase the flexibility of electronic devices because the rechargeable power does not require the connection of cables and batteries. The energy used in the electromagnetic 950 MHz implies one of the frequencies of the wireless network en masse in the room. The objection in this research is to find out how to design an SRR that has a resonant frequency of around 950 MHz, and how to know its characteristics. Based on previous research, variations were carried out with three measurement parameters which were carried out separately and simulated using CST software to achieve a resonant frequency of 950 MHz. The results of the simulation and design process with CST software are three SRR models which are then named SRR 1, SRR 2, and SRR 3. SRR 1 has a ring width 5.6 mm, a slit width 2.7 mm, a ringside length 35 mm, and a ring plate thickness 0.017 mm. SRR 2 has 2.9 mm in a ring width, 10.8 mm in a slit width, 35 mm in a ringside length, and 0.017 mm in a ring plate thickness. SRR 3 has a ring width 2.9 mm, a slit width of 2.7 mm, a ringside length of 32.25 mm, and a ring plate thickness of 0.017 mm. SRR is expected to obtain energy from wireless network energy that is often used indoors.

Keywords: *Split Ring Resonator, microwave, resonant frequency, CST, energy harvesting*

INTRODUCTION

Wireless technology has long been discovered, but so far its use only as an electromagnetic signal capture. Recently, antenna technology has shown good development, especially in terms of the efficiency of electromagnetic energy absorption. This increase was seen when the split ring resonator (SRR) was introduced. SRR utilizes the inductive and capacitive properties arising from the structural design so that it has a certain resonant frequency. With these properties, SRR has a higher efficiency and resonance properties are easier to adjust. Due to the latter property, SRR can be used to design metamaterials that have certain unique properties to electromagnetic waves, such as permittivity and negative permeability [1-3]. Currently, many studies have been carried out with different configurations of SRR, namely, circular SRR (C-SRR), square SRR (S-SRR), hexagonal SRR (H-SRR), and so on, where intensively, circular SRR and square has been reported [4-10].

SRR is usually used in many designs such as antennas [11-12] (in this case it is used to reduce the size of the antenna [13-17]), and to suppress harmonics generated by rectifier circuits [18]. A small electrical rectena operating at 1.5754 GHz was designed by Zioalkowski et al, at the

University of Arizona by utilizing a structure inspired by metamaterials. Rectenna is a system that harvests and converts the surrounding RF energy into DC power through an antenna which is followed and matched by a rectifier circuit and a resistive load. This structure can reduce the total size of the rectal system when operating at low frequencies drastically. This is particularly useful for applications that demand a small size of the rectal system, which was a problem with the previous rectal [19-24]. Meanwhile, the research conducted by Wang et al (2019) focused their study on the harvesting of single-frequency ambient energy, which is mostly 2.45 GHz [25], as it is less affected by air attenuation.

Furthermore, WSN (wireless sensor network) technology can be run without additional power supply. In 2011 a comparative study was carried out by Saha and Siddiqui (2011) for three double-SRR [20]. However, this study was only conducted for single SRR. Recently, it has been shown that a 3D square SRR of finite height can exhibit much stronger coupling compared to full planar structures with the same footprint. The coupling coefficient is also increased to increase the height of the resonator. This can be leveraged to design devices featuring a wider operating bandwidth or mini-layouts without performance degradation [26].

This study utilizes the square SRR as a harvester of electromagnetic energy in microwaves, and explain how to design SRR so that it can capture electromagnetic energy at a frequency of 950 MHz, because by utilizing energy in this frequency range, the energy emitted is not only wasted but can be used as a power source.. The nature and characteristics of the SRR are described in more detail. The properties and characteristics that want to be known are those related to changes in the size of the gap width, conductor width, and length of the SRR, and will be simulated on CST software. By knowing the characteristics of the SRR that has been made, a proper electromagnetic energy harvester can be made. When the selected frequency is 950 MHz, the energy obtained can be obtained from the energy of the wireless network that is often used in the room. Thus, the WSN system can operate without additional power supply. In WSN, the scenario of power usage obtained from SRR is used for device sensors that do not transmit or work continuously. This is because the power per unit time obtained from the SRR is quite small so that in order to be used to transmit communication signals, the power must be collected first in a certain time span.

METHODS

The previous SRR model was obtained from research conducted by [27], as shown in Table 1, which will be simulated on CST software, had a ring width of 2.9 mm, a slit width of 2.7 mm, a ringside length of 35 mm, and a ring plate thickness of 0.017 mm. After the model has been designed in the software and the simulation results have been obtained, three SRR parameters are changed in this study: slit width, copper ring width, and copper ring length and simulated until the SRR has a frequency response of 950 MHz. This is varied in different experiments, so that there are three design results obtained.

Table 1. SRR Design Size Reference [27].

Reference	Ring Width (mm)	Slit Width (mm)	Ringside Length (mm)	Ring Plate Thickness (mm)
Wang et al (2015)	2.9	2.7	35	0.017
SRR 1	5.6	2.7	35	0.017
SRR 2	2.9	10.8	35	0.017
SRR 3	2.9	2.7	32.25	0.017

Design and Simulation Method

Simulation of the SRR model was carried out using CST software. The menu selected on the initial display is MW & RF & Optical because the equipment we want to simulate operates at a microwave frequency of around 950 MHz. On the next menu select the Periodic Structure menu, so that three workflow options appear. Because SRR is included in the metamaterial and the simulation we need to do is for a single SRR unit, select the label Metamaterial – Full structure. Next, the solver option will appear for the simulation we need. There is a choice of Time Domain and Frequency Domain. Then select the Time Domain menu to run. When we enter the design board and want to simulate, we choose the solver to run again. This initial selection menu is only to show what solvers can be run and the simulation objectives that we will choose in the design. Next are the unit panels that will be selected in the design we create. In this study, the following units were selected: mm (millimeter) for dimensions, MHz (megahertz) for frequency, ns (nanosecond) for time, Kelvin for temperature, V (volt) for voltage, A (ampere) for current, Ohm for resistance, S (siemen) for conductance, nH (nano henry) for inductance, and pF (piko farad) for capacitance.

The determination of the minimum and maximum frequency ranges of the simulation to be carried out is selected in frequency or in wavelength. In addition, there are also several choices of terrain and what magnitudes can be monitored. For the simulation to be carried out, we choose a range using the frequency scale, which is between 0 to 6000 MHz. Although the intended frequency is 950 MHz, the initial design of the model made is most likely outside the 950 MHz frequency. So a wider frequency range is chosen.

Once the template has been created, a board for creating a three-dimensional tool design will appear. Some various menus and options can be used to design the SRR to be made. On the design board, the first step to start the design is to determine the basic parameters of the SRR. These parameters include slit width, ring plate thickness (SRR thickness), ringside length (SRR length), ring width (SRR width), PCB material side length (substrate length), and PCB material thickness (substrate thickness). The whole process in modeling is presented in Figure 1.

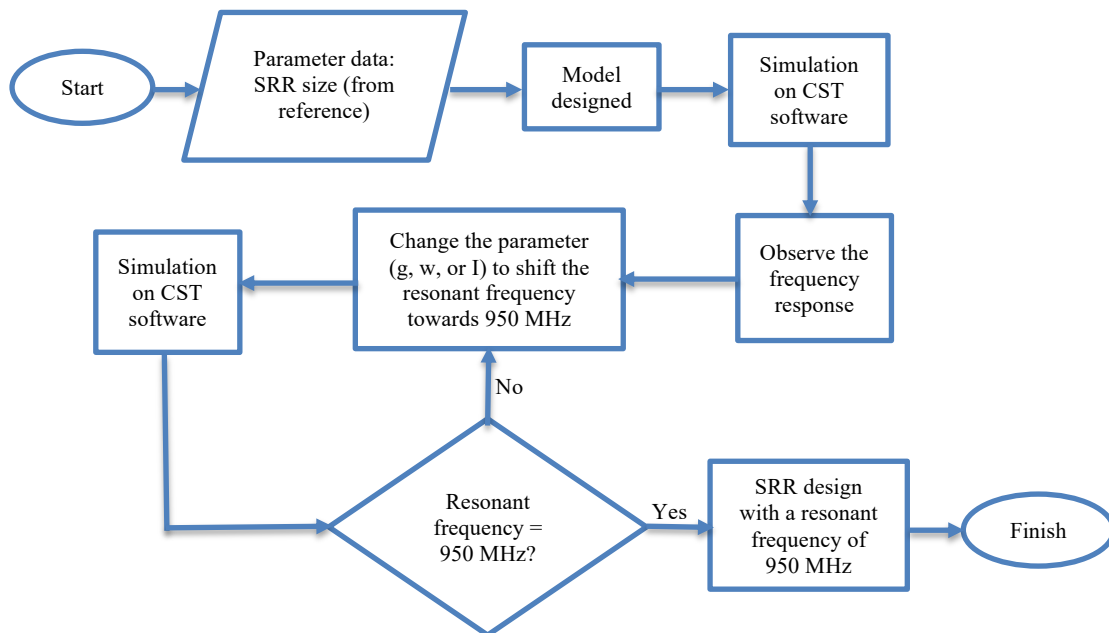


Fig. 1. Flowchart of Proposed Model

After defining the parameters, the SRR modeling can be started. First, the model of the PCB board used is made. The board is in the form of a box with a thickness of 1.6 mm and a side length of 40 mm as defined previously. Then go to the modeling menu then select the brick column. The shape to be created will be defined using Cartesian coordinates. So for PCB boards with FR-4 material and a side length of 40 mm and a thickness of 1.6 mm.

The next is to make a copper plate as an SRR which will later be in the form of a split ring as the name implies. The steps that need to be taken to make rings are the same as when making PCB boards (substrate) but with different sizes and positions. The length of the outer ring to be made is 35 mm. This length has been defined previously as the SRR length which is given the symbol l . And the thickness of the copper plate is 0.017 mm which is symbolized by w .

To make a hole in the center of the copper plate so that it is shaped like a ring, we need to do the next steps. Open the modeling menu then select the brick column as before, then create a smaller copper plate inside the previous copper plate. To get a ring width of w , then the X_{\min} and Y_{\min} columns are filled with $-(l/2)+w$ while the X_{\max} and Y_{\max} columns are filled with $(l/2)-w$. The thickness is made like the thickness of the previously made copper plate, which is h . For the same material selected from copper.

To punch holes in a larger copper plate so that it forms a ring, the trick is to subtract the first plate from the second plate. In the left menu, open the component1 icon, then select the first plate that was created earlier. Then open the Boolean option in the menu above and select Subtract. After that click the second plate that we have created in the menu on the left, then enter. Then the second plate will subtract the first plate, so the copper plate is now in the form of a ring. After that, the results of the subtraction of the first plate with the second plate will be displayed. The ring formed is a square with a width according to the parameter w , which is 2.9 mm.

To create a slit in the ring, it is necessary to move the coordinate center at the location where the slit will be made. This can be done with the local WCS (Working Coordinate System) option in the modeling options on the top menu. Then select Align WCS and attach it to the side of the ring where the gap will be made. After that make a small copper plate as big as the desired gap. To make the gap width equal to the parameter g , enter the values in Figure 2.

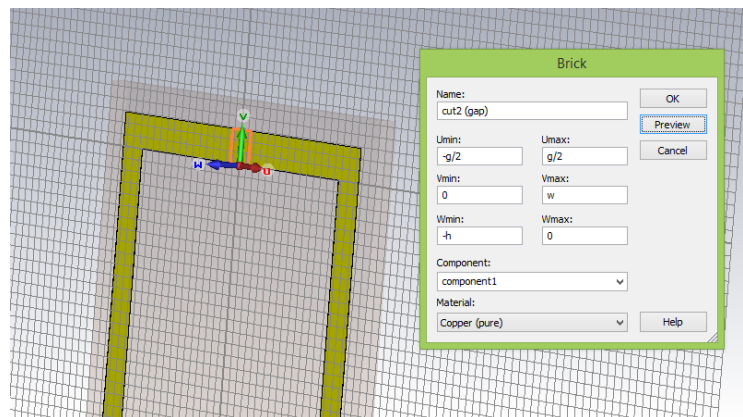


Fig. 2. Remove a Little Part of Ring to make a gap

Next is to subtract the copper plate that was first made (which is already in the form of a ring) with the smaller plate that is in the place of the gap. The method of subtracting is the same as the method of making ring holes that have been described previously, namely using the Boolean menu and then Subtracting. After that, it can be seen the overall appearance of the front view of the SRR model that has been made. Furthermore, the model in this CST software can be simulated to see its characteristics.

Before the simulation is carried out, several things need to be set so that the simulation runs as desired. One of them is the simulated frequency range. Because the target frequency is 950 MHz and the possible initial frequency obtained is greater than that, the frequency range is set around that frequency. Here the selected frequency range from 0 to 6000 MHz.

When setting the boundaries of the area or volume where the simulation is carried out. In CST software this can be set in the Background Properties menu. The boundaries are set as a cube with sides along l_s , which is the same as the side length of the PCB board that is made. After that, setting the boundary conditions or Boundary Condition. This Boundary Condition setting is in the Simulation option on the top menu. Because electromagnetic waves want to be emitted from the right or left (X_{\min} and X_{\max}) so that the magnetic field can be adjusted in the front and back directions (Z_{\min} and Z_{\max}) and the electric field can be set in the up and down directions (Y_{\min} and Y_{\max}). The magnetic field is set in the front and back directions (Z_{\min} and Z_{\max}) with the intention that the magnetic field can penetrate the SRR in a perpendicular direction to cause an electromotive force (emf) on the SRR. To set the boundary conditions as desired, fill in the X_{\min} and X_{\max} fields with open options, Y_{\min} and Y_{\max} with electric options, and Z_{\min} and Z_{\max} with magnetic options.

Another thing that needs to be set before doing the simulation is setting the Waveguide Port. The waveguide port is the terminal where signals are transmitted and received back. Because we want electromagnetic waves to be emitted from the right and left (X_{\min} and X_{\max}), two ports are installed in the X_{\min} and X_{\max} planes. The settings and placement of Port 1 in the X_{\min} field can be seen in Figure 3. As for the arrangement and placement of Port 2 in the X_{\max} field, so that it is in the X_{\max} field, the Normal option is still placed on X but the Orientation is selected in the Negative option.

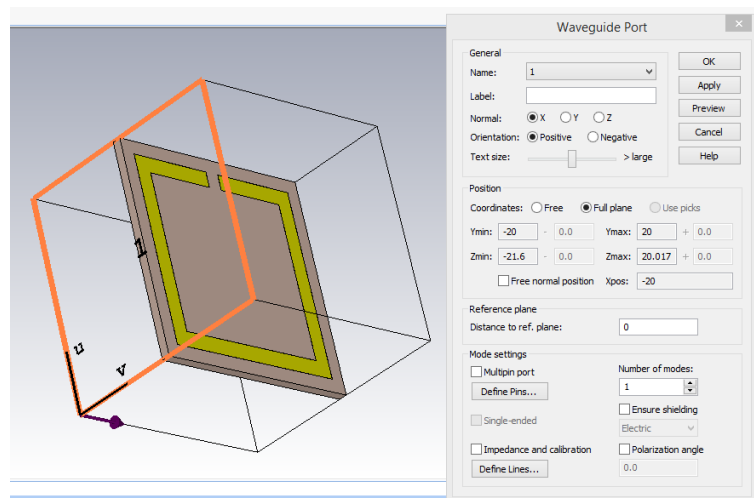


Fig. 3. Installing port 1 on the side of SRR.

After everything has been set correctly, the simulation can start. Simulation in CST software can be done by running the Setup Solver menu in the Simulation option at the top. Because at the beginning of the settings menu the time domain solver is selected, what will appear on the Solver Setup menu is also the time domain solver. Although actually at this stage we can choose another type of solver, for this simulation we are using a time-domain solver to get the desired results, then on the Time Domain Solver Parameters menu, we choose the level of accuracy, source type, S-parameter settings, and others.

RESULT AND DISCUSSIONS

CST software is used in the design process and simulation of the created SRR. The initial design before the simulation was carried out was in the form of an SRR model that had been previously developed by [27]. After the simulation, this SRR has a resonant frequency at 835 MHz. Thus the resonant frequency of the SRR is not yet reached the desired frequency, which is 950 MHz.

Design with Variations in Ring Width

After seeing the results of the initial simulation, the SRR parameter was resized. First, make changes to the ring width or parameter w . Then the simulation is done and the resonance frequency is seen. If the resonant frequency has not reached 950 MHz, the parameter changes are made again. Then do a simulation and see if the resonant frequency has reached 950 MHz until it reaches 950 MHz. The display of the simulation results on the scheme of changing the width of the ring can be seen in Figure 4.

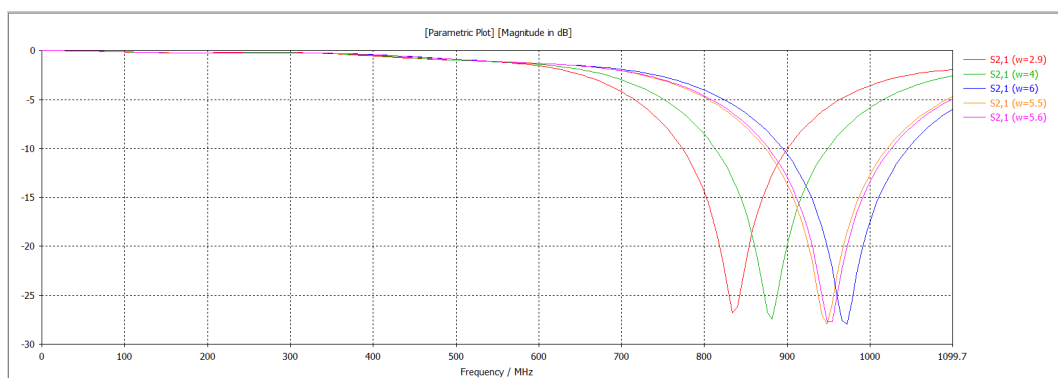


Fig. 4. Graph S_{21} of the simulation results of ring width variations.

Figure 4 concluded that with a change in the slit width, the resonant frequency of the SRR will shift. The result shows that the width of the gap in the design makes the resonant frequency higher. The split ring resonator utilizes the inductive nature of the copper ring and the capacitive nature of the gap to produce a resonant frequency. Resonant frequency occurs when the capacitive reactance has the same value as the inductive reactance. The reactance value changes when the size of the SRR is changed. Increasing the size of the ring width with a fixed outer ring length causes the area covered by the conductor ring to decrease. When the SRR is analogous to a solenoid inductor with $N = 1$, the reduced area covered causes the inductance value to decrease according to the equation 1.

$$L = \frac{\mu_0 \mu_r K N^2 A}{l} \quad (1)$$

where L is the inductance value, μ_0 is the vacuum permeability, μ_r is the relative permeability of the material inside the solenoid. K is the Nagaoka coefficient, N is the number of turns, A is the cross-sectional area of the solenoid, and l is the length of the solenoid. The reduced inductance value makes the SRR resonant frequency increase as illustrated in equation 2.

$$f = \frac{1}{2\pi\sqrt{LC}} \quad (2)$$

where f is the resonant frequency in Hertz, L is the inductance in Henrys, and C is the capacitance in Farad. The larger the ring width, the higher the resonant frequency. To see the value of the resonant frequency from the simulation results, it is shown in Figure 5.

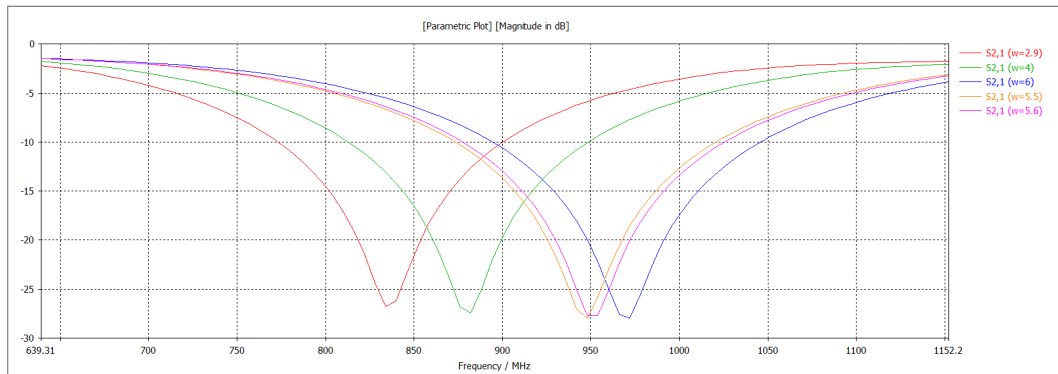


Fig. 5. The graph of the peak response of S_{21} from variations in ring width.

It can be observed that when the ring width is 2.9 mm the resonant frequency is 835 MHz, for a ring width of 4 mm the resonant frequency is 880 MHz, and for a ring width of 5.5 mm, the resonance frequency is 947 MHz, while for a ring width of 6 mm resonant frequency 970 MHz. Now it can be seen that a resonant frequency of 950 MHz can be achieved when the ring width is 5.6 mm. The relation of ring width and the resulting resonant frequency is shown in Figure 6.

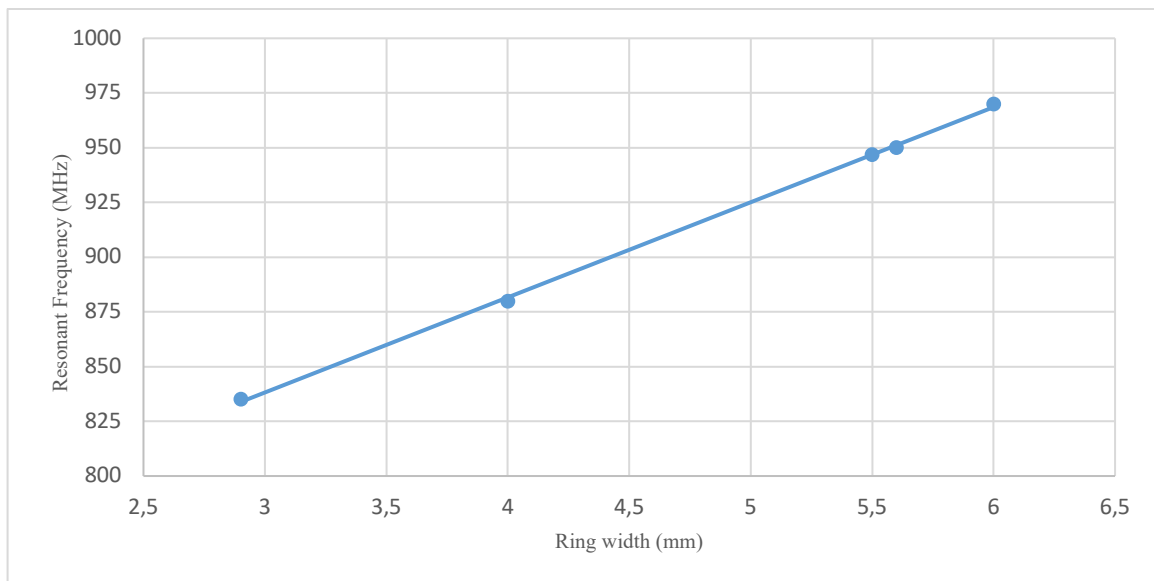


Fig. 6. The graph of the relation of ring width and resonant frequency.

After a redesign with a ring width of 5.6 mm, the results are shown in Figure 7. The SRR model with this design is hereinafter referred to as the SRR 1 model.

Design with Variations in Slit Width

Starting from the design with the size as shown in the initial parameters, variations are made by changing the value of the gap width, namely g , to 2.7 mm, 4 mm, 7 mm, 10 mm, 13 mm, and 10.8 mm. Simulations are performed from a frequency of 0 MHz to 6000 MHz. The frequency response graph show in Figure 8.

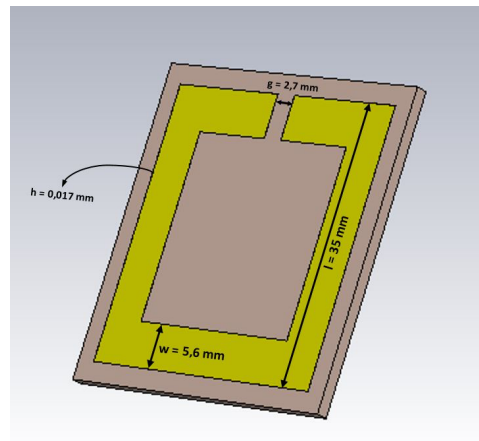


Fig. 7. SRR 1 model display (ring width 5.6 mm).

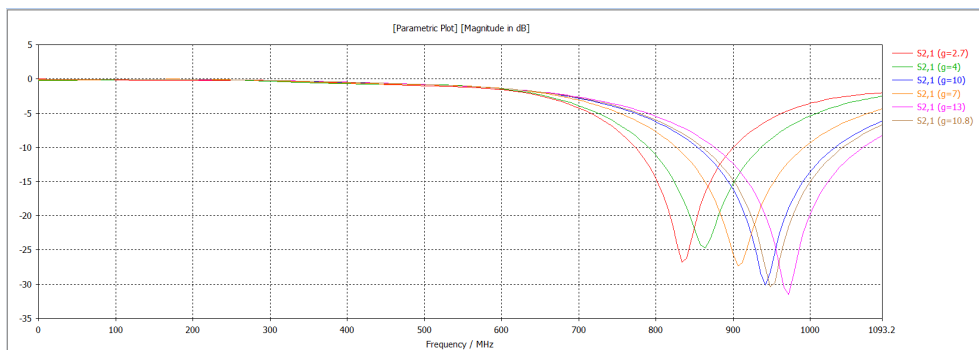


Fig. 8. Enlarged S_{21} graph of the variation of the gap width.

It shows that the increase in the SRR slit width makes the resonant frequency higher. This is related to the capacitive nature of the SRR. When the inductive reactance and capacitive reactance of the SRR at a certain frequency are the same, resonance occurs as formulated in equation 2. As the slit width in the SRR increases, there will be an increase in the distance between the conductor plates in the gap. The wide distance between the conductor plates in the capacitor will reduce the capacitance value. This is shown in the equation 3.

$$C = \epsilon_0 \epsilon_r \frac{A}{d} \quad (3)$$

where ϵ_0 is the vacuum permittivity or dielectric constant and ϵ_r is the dielectric constant of the material between the plates. So it can be seen that the amount of capacitance in a capacitor is influenced by the area of the conductor plate (A) and the distance between the two conductors (d). As in the case of capacitors, this causes the value of the SRR capacitance to get smaller. Based on equation 2, A small capacitance value will increase the resonant frequency. This can explain the results showing that the width of the gap in the design will increase the resonant frequency. To find out the value of each resonant frequency, we need to magnify the graph in Figure 7. The results of this magnification are shown in Figure 9.

The graph in Figure 9 shows that for a slit width of 2.7 mm the resonance frequency is 835 MHz, for a slit width of 4 mm the resonance frequency is 865 MHz, while for a slit width of 7 mm the resonance frequency is 910 MHz, for a slit width of 10 mm the resonance frequency is 942 MHz, and for a slit width of 13 mm the resonant frequency is 972 mm. From these results it can be seen that the resonant frequency of 950 MHz is in the slit width between 7 mm and 13 mm. So we



know that the resonant frequency of 950 MHz is obtained when the slit width is 10.8 mm. The effect of the slit width on the resonant frequency generated by the SRR based on the simulation is shown in the graph in Figure 10.

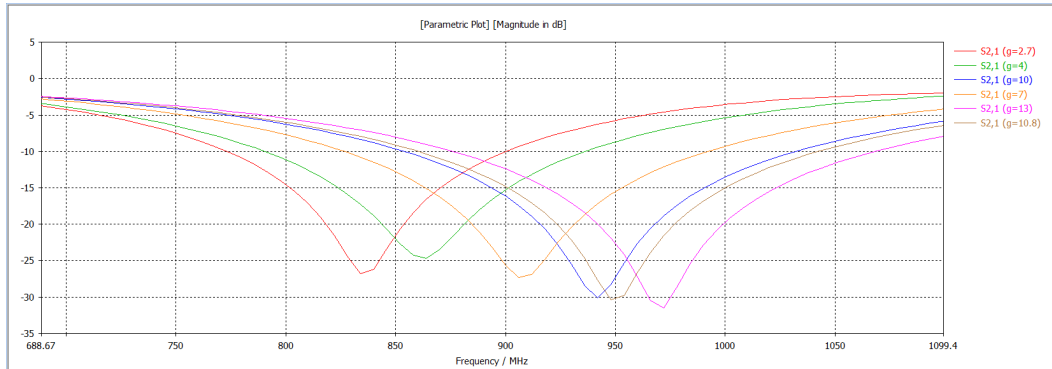


Fig. 9. The graph of the peak response of S_{21} from the variation of the slit width.

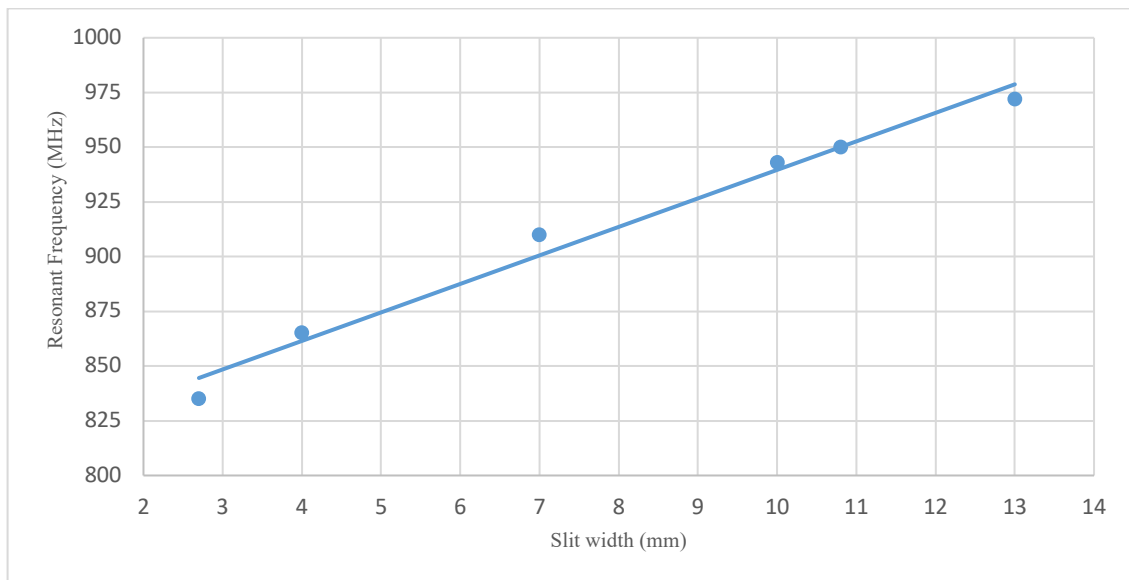


Fig. 10. Graph of the relation of slit width and resonant frequency.

Based on the value of the gap width obtained through the simulation, which is 10.8 mm, an SRR design is made which has a size of $g = 10.8$ mm; $w = 2.9$ mm; $l = 35$ mm; and $h = 0.017$ mm. The display of the SRR model in CST software with this design can be seen in Figure 11. Furthermore, this SRR model is called the SRR 2 model.

Designs with Variations in Side Ring Length

As with previous simulations and designs, the design starts from the model given in the initial parameters, varying the ringside length value and simulation until it reaches a resonant frequency value of 950 MHz. The side length of the ring is varied with values of 35 mm, 32 mm, 30 mm, 32.5 mm, 32.2 mm, and 32.25 mm. After simulation, the frequency response graph can be observed in Figure 12.

Figure 12 shows the simulation results of the frequency response at a frequency of 0 MHz to 6000 MHz. The deepest frequency response is indicated at frequencies around 900 MHz. So to better understand the effect of changing the ring length on the frequency response, the graph must be enlarged.

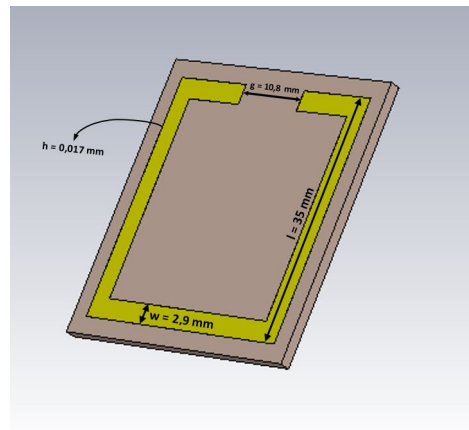


Fig. 11. SRR 2 model display (slit width 10,8 mm).

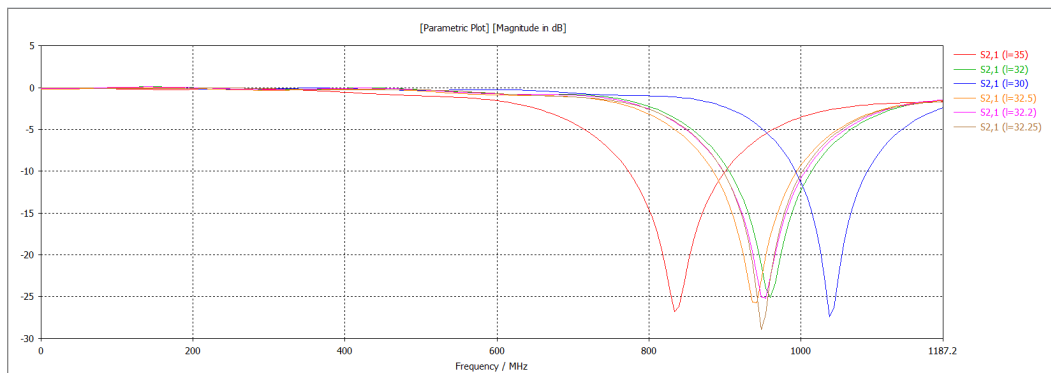


Fig. 12. Graph of S_{21} simulation results of ring length variations.

Figure 12 shows that variations in ring length affect the resonant frequency, a small ring will lower the resonant frequency. SRR has capacitive and inductive properties due to its construction (equation 1). The equation explains that the inductance value of an inductor in the form of a solenoid is influenced by the relative permeability of the material inside the solenoid, the number of turns, the length of the solenoid, and the cross-sectional area of the solenoid.

The SRR made is analogous to a solenoid with $N = 1$. The larger the side length of the SRR, the greater the cross-sectional area so that the inductance value will increase. Conversely, if the length of the SRR side is getting smaller, the cross-sectional area will decrease and the inductance value will decrease. Based on equation 2, The small value of the inductance in the circuit will increase the resonant frequency. This explains why so possible to increase the resonant frequency of the SRR by reducing the side length of the SRR. To determine the magnitude of the resonant frequency, it is necessary to re-magnify as shown in Figure 13.

At the ringside length of 35 mm, the resonant frequency is at a frequency of 835 MHz. When the ringside length is changed to 32 mm, the resonant frequency is at 959 MHz. Meanwhile, with a ringside length of 30 mm, the resonance frequency is higher at a frequency of 1040 MHz. Since the target frequency is 950 MHz, the side length is made slightly longer than 32 mm. At the ringside length of the 32.5 mm the resonant frequency is 940 MHz, so it needs to be readjusted a bit to reach 950 MHz. After taking the values carefully, the resonance frequency of 950 MHz was obtained when the ringside length was 32.25 mm. Based on the results, the relation of the ringside length and the SRR resonant frequency can be depicted in a graph in Figure 14.

After obtaining the appropriate ringside length values, the SRR model in CST is obtained as shown in Figure 15. The SRR model with this design is hereinafter named the SRR 3 model.

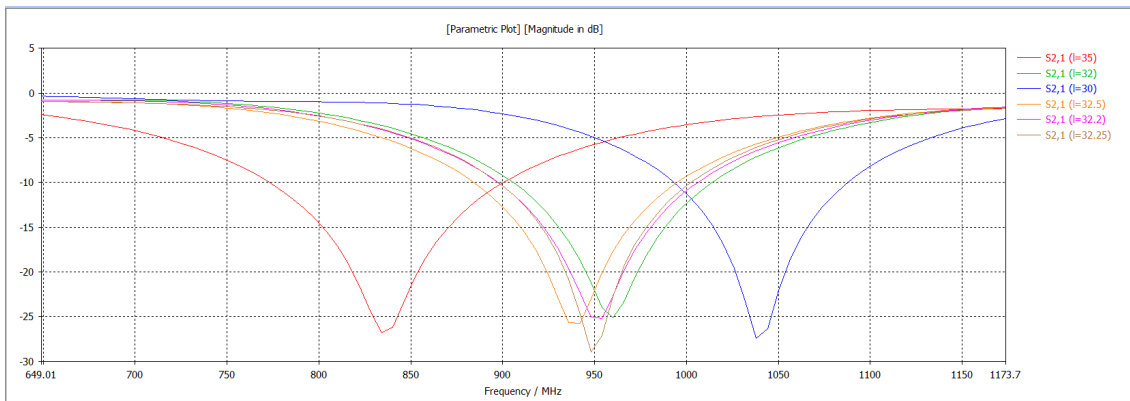


Fig. 13. The graph of the peak response of S_{21} from variations in ring length.

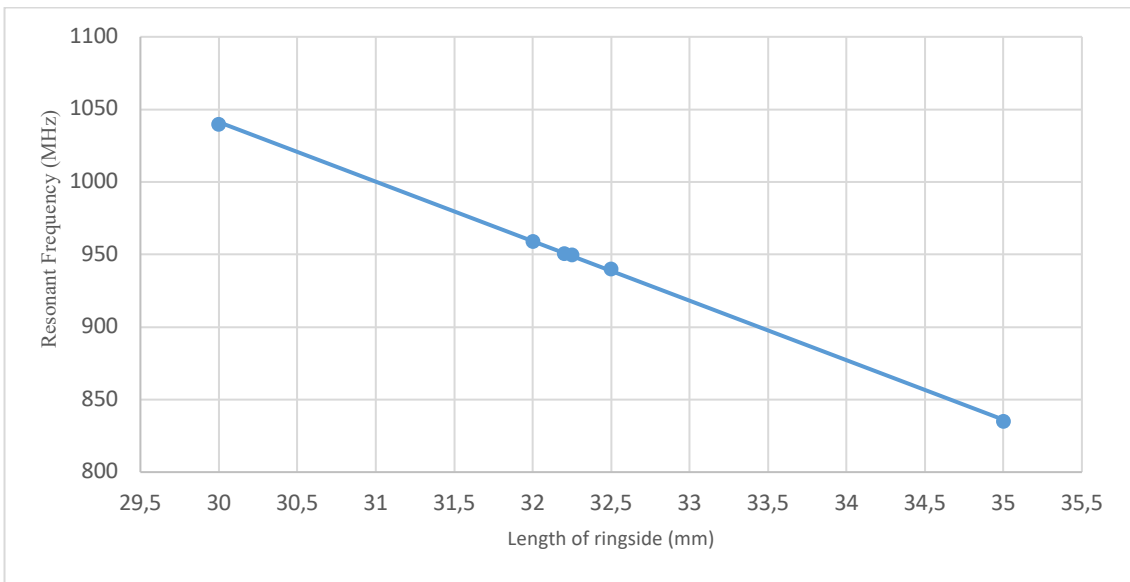


Fig. 14. Relation of the length of the ringside and the resonant frequency.

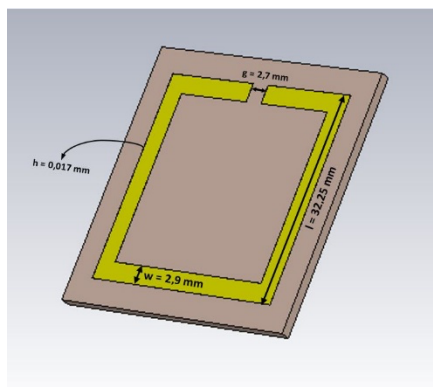


Fig. 15. SRR 3 model display (ringside length 32,25 mm).

CONCLUSIONS

This research was conducted to obtain an SRR design capable of working at a resonant frequency of 950 MHz. The design begins with conducting a design simulation using CST software. The dimensions of the initial design of the SRR were based on the model previously developed by Wang et al [27] with sizes of 2.9 mm, 2.7 mm, 35 mm, and 0.017 mm which described the value of ring width, slit width, ringside length, and thickness of the ring plate. Based on the simulation results, the design is only able to work at the resonant frequency of 835 MHz, so adjustments need to be made, where the adjustments are 5.6 mm ring width, 10.8 mm slit width, and 32.25 mm ringside length. Based on the simulation results in this design, the dimensions of the SRR with these values are able to work at a resonant frequency of 950 MHz. The simulation is done by setting one parameter as the independent variable while the other two parameters as the controlled variable.

Then this design made into a prototype based on the simulation results. The SRR prototype design is made in three forms: SRR 1, SRR 2, and SRR 3. SRR 1 has ring width 5.6 mm, slit width 2.7 mm, ringside length 35 mm, and ring plate thickness 0.017 mm. SRR 2 has 2.9 mm in ring width, 10.8 mm in slit width, 35 mm in ringside length, and 0.017 mm in ring plate thickness. SRR 3 has a ring width 2.9 mm, a slit width of 2.7 mm, a ringside length of 32.25 mm, and a ring plate thickness of 0.017 mm. Further research is expected to conduct a comprehensive analysis of the dimensions and materials of the SRR and carry out an analysis related to the use of double SRR.

REFERENCES

- [1] Karthikeyan, S. S and Arulvani, M, "Double negative metamaterial design using open split ring resonator", *2010 IEEE Students Technology Symposium (TechSym)*, Kharagpur, pp. 142-145, 2010. DOI: <https://doi.org/10.1109/TECHSYM.2010.5469222>
- [2] Vaseleto, V. G, "The Electrodynamics of Substances with Simultaneously Negative Value ϵ and μ ", *Physics-Uspokhi*, vol. 10, Num. 4, pp. 509-514, 1968. DOI: [10.1070/PU1968v010n04ABEH003699](https://doi.org/10.1070/PU1968v010n04ABEH003699)
- [3] Islam, Md. R, Islam, M. T, Soliman, M. S, Baharuddin, M. H, Mat, K, Moubark, A. M, and Almalki, S. H. A, "Metamaterial Based on an Inverse Double V Loaded Complementary Square Split Ring Resonator for Radar and Wi-Fi Applications", *Scientific Report*, 21782, pp. 1-19, 2021. DOI: <https://doi.org/10.1038/s41598-021-01275-6>
- [4] Pendry, J. B., Holden, A. J., Ribbins, D. J., and Stewart, W. J, "Magnetism from Conductors and Enhanced Nonlinear Phenomenon", *IEEE Trans. Microwave Theory Tech*, vol. 47, Issue 11, pp. 2075 – 2084, 1999. DOI: <https://doi.org/10.1109/22.798002>
- [5] Marquez, R., Medina, F, and Rafii-El-Idrissi, "Role of Bianisotropy in Negative Permeability and Left-handed Metamaterials", *Phys. Rev. B*, Vol. 65, issue 14, pp. 1-6, 2002. DOI: <https://doi.org/10.1103/PhysRevB.65.144440>
- [6] Ziolkowski, R. W, "Design, Fabrication, and Testing of Double Negative Metamaterials", *IEEE Trans. Antennas Propagat*, pp. 2572 – 2581, Vol. 51, Issue 7, 2003. DOI: [10.1109/TAP.2003.813622](https://doi.org/10.1109/TAP.2003.813622)
- [7] Marquez, R, Meza, F, Martel, J, Medina, F, "Comparative Analysis of Edge- and Broadside-Coupled Split Ring Resonators for Metamaterial Design-Theory and Experiment", *IEEE Trans. Antennas Propagat*, Vol. 51, Issue 10, pp. 2572 – 2581, 2003. DOI: [10.1109/TAP.2003.817562](https://doi.org/10.1109/TAP.2003.817562)
- [8] Saha, C., and Siddiqui, J. Y, "Versatile CAD Formulation for Estimation of the Resonant Frequency and Magnetic Polarizability of Circular Split Ring Resonators", *International Journal of RF and Microwave Computer Aided Engineering*, Vol. 21, Issue 4, pp. 432-438, 2011. DOI: <https://doi.org/10.1002/mmce.20533>

- [9] Lim, S., Caloz, C., and Itoh, T, “Electronically Scanned Composite Right/Left Handed Microstrip Leaky-wave Antenna”, *IEEE Microwave Wireless Comp. Lett.*, Vol. 14, Issue 6, pp. 277 – 279, 2004. DOI: [10.1109/LMWC.2004.828008](https://doi.org/10.1109/LMWC.2004.828008)
- [10] Saha, C., and Siddiqui, J. Y, “Simplified CAD Model for Accurate Estimation of the Resonant Frequency of Edge Coupled Hexagonal Split Ring Resonators”, *Proc. APSYM 10, Cochin*, Vol. 21, No. 4, pp. 432-438, 2010. DOI: [10.1002/mmce.20533](https://doi.org/10.1002/mmce.20533)
- [11] Ezanuddin, A. A. M., Malek, F, and Soh, P. J, “Investigation of Complementary Split Ring Resonator with Dielectric Ring”, *Loughborough Antennas and Propagation Conference (LAPC)*, pp. 297 – 300, 2010. DOI: [10.1109/LAPC.2010.5665999](https://doi.org/10.1109/LAPC.2010.5665999)
- [12] Majid, H. A., Rahim, M., and Masri, “T. Left Handed Metamaterial Design for Microstrip Antenna Application”, *IEEE International RF and Microwave Conference (RFM 2008)*, pp. 218 – 221, 2008. DOI: [10.1109/RFM.2008.4897426](https://doi.org/10.1109/RFM.2008.4897426)
- [13] Zhu, N and Ziolkowski, R. W, “Metamaterial-inspired, Near-field Resonant Parasitic Gps Antennas: Designs and Experiments”, *Antennas and Propagation (APSURSI), IEEE International Symposium*, pp. 658—660, 2011. DOI: [10.1109/APS.2011.5996797](https://doi.org/10.1109/APS.2011.5996797)
- [14] Nornikman, H., Ahmad, B. H., Abd Aziz, M. Z. A, and Othman, A. R, “Effect of Single Complimentary Split Ring Resonator Structure on Microstrip Patch Antenna Design”, *IEEE*, pp. 239 – 244, 2012. DOI: [10.1109/ISWTA.2012.6373852](https://doi.org/10.1109/ISWTA.2012.6373852)
- [15] Jahangiri, M., and Rajebi, S, “Effects of Split Ring Resonator (SRR) Metamaterial on the Radiation Pattern and Variation of the Heating Focus Point of the Microstrip Patch Antenna”, *ASTES, Advances in Science, Technology and Engineering Systems Journal*, Vol. 5, No. 1, pp. 307 – 316, 2020. DOI: <https://dx.doi.org/10.25046/aj050139>
- [16] Rashid, A. H. A., Hassan, N., Azizi, M. S. N, Ramli, M. H, “Bow-Tie Patch Antenna with Different Shaped of Complementary Split Ring Resonator (SRR) Structures”, *Journal of Telecommunication, Electronic and Computer Engineering. UteM Open Journal*, Vol. 9, No. 1-3, pp. 41 – 45, 2015.
- [17] Ohi, Md. A. R, Hasan, Z, Bin Faruquee, S. F, Kawsar, A. A. M, Ahmed, A, “Wideband Minkowski Fractal Antenna using Complementary Split Ring Resonator in Modified Ground Plane for 5G Wireless Communication”, *Engineering Reports*, Vol. 3, Issue 9, pp. 1-12, 2021. DOI: <https://doi.org/10.1002/eng2.12388>
- [18] J. Hansen, C.H. Ahn, and Chang, K, “A 5.8 GHz High gain, Aperture Coupled Rectenna Utilizing a *Split Ring Resonator Filter*”, *Antennas and Propagation Society International Symposium (APSURSI), 2010 IEEE*, pp. 1-4. IEEE, 2010. DOI: [10.1109/APS.2010.5561185](https://doi.org/10.1109/APS.2010.5561185)
- [19] Zhu, N, Ziolkowski, R. W, and Xin, H, “A Metamaterial-inspired, Electrically Small Rectenna for High-efficiency, Low Power Harvesting and Scavenging at the Global Positioning System L1 Frequency”, *Applied Physics Letters*, Vol. 99, Issue 11, pp. 1-3, 2011. DOI: <https://doi.org/10.1063/1.3637045>
- [20] Saha, C., and Siddiqui, J. Y, “A Comparative Analysis for Split Ring Resonators of Different Geometrical Shapes”, *IEEE*, pp. 1-4, 2011. DOI: [10.1109/AEMC.2011.6256871](https://doi.org/10.1109/AEMC.2011.6256871)
- [21] Ren, Y. J, Farooqui, M. F, and Chang, K, “A Compact Dual-frequency Rectifying Antenna with High-orders Harmonic-rejection”, *Antennas and Propagation, IEEE Transactions on*, Vol. 55, Issue 7, pp. 2110-2113, 2007. DOI: [10.1109/TAP.2007.900275](https://doi.org/10.1109/TAP.2007.900275)
- [22] Suh, Y. H and Chang, K, “A High-efficiency Dual-frequency Rectenna for 2.45-and 5.8-GHz Wireless Power Transmission”, *Microwave Theory and Techniques, IEEE Transactions on*, Vol. 50, Issue 7, pp. 1784—1789, 2002. DOI: [10.1109/TMTT.2002.800430](https://doi.org/10.1109/TMTT.2002.800430)
- [23] Heikkinen, J and Kivikoski, M, “A Novel Dual-frequency Circularly Polarized Rectenna”, *Antennas and Wireless Propagation Letters, IEEE*, Vol. 2, pp. 330—333, 2003. DOI: [10.1109/LAWP.2004.824166](https://doi.org/10.1109/LAWP.2004.824166)
- [24] Benayad, A, and Tellache, M, “A Compact Energy Harvesting Multiband Rectenna Based on Metamaterial Complementary Split Ring Resonator Antenna and Modified Hybrid Junction

- Ring Rectifier”, *International Journal of RF and Microwave Computer Aided Engineering*, Vol. 30, Issue 2, pp. 1-11, 2019. DOI: <https://doi.org/10.1002/mmce.22031>
- [25] Wang, L, Yang, L, Fan, Y, Shen, M. Li. Y, and Shi, Y, “A Compact Omnidirectional Dual-Circular Rectenna for 2.45 GHz Wireless Power Transfer”, *International Journal of RF and Microwave Computer-Aided Engineering*, Vol. 29, Issue 1, pp. 1-7, 2018. DOI: <https://doi.org/10.1002/mmce.21625>
- [26] Vallecchi, A, Stevens, C, and Shamonina, E, “3D Coupled Resonators for Enhanced Filter Design”, *12th European Conference on Antennas and Propagation (EuCAP 2018)*, London, pp. 128-131, 2018. DOI: 10.1049/cp.2018.0487
- [27] Wang, X, Zhao, Z, Chen, K, He, F, Yuan, L, and Lu, T, "Numerical Studies on Dual-band Electromagnetic Energy Harvesting with Double-ring Split-Ring Resonators", *2015 50th International Universities Power Engineering Conference (UPEC)*. Stoke on Trent, pp. 1-5, 2015. DOI: [10.1109/UPEC.2015.7339836](https://doi.org/10.1109/UPEC.2015.7339836)